Rev. Adv. Mater. Sci. 43 (2015) 61-66

MICROSTRUCTURE AND TEXTURE HOMOGENEITY OF ECAP TITANIUM

Alexander Zhilyaev[1,2], Nikolay Parkhimovich[1], Georgy Raab[3], Vladimir Popov[1] and Valery Danilenko[1]

[1]Institute for Metals Superplasticity Problems, Russian Academy of Science, Khalturina, 39, Ufa, 450001 Russia
[2]Research Laboratory for Mechanics of New Nanomaterials,
Peter the Great St. Petersburg Polytechnic University, Polytechnicheskaya 29, St. Petersburg, 195251, Russia
[3]Institute of Physics of Advanced Materials, Ufa State Aviation University, K. Marx, 12, 45000 Ufa, Russia

Received: October 21, 2015

Abstract. Microstructure and texture of commercially pure titanium subjected to eight passes by equal channel angular pressing via route Bc at temperature 450 °C have been thoroughly analyzed by transmission electron microscopy (TEM), X-ray diffraction and microhardness mapping in flow and top planes and cross section of the billet. Unlike previously published reports some inhomogeneity (i.e. non-equiaxiality of grains) of fine structure has been detected by careful TEM inspection. Texture results have supported that during ECAP pressing at elevated temperature mostly pyramidal slip systems were active.

1. INTRODUCTION

Titanium is an important metal for high performance structural applications [1]. Mostly two parameters, namely texture and mean grain size, have a major effect on physical and mechanical properties. Actually both parameters are interrelated [2] and need to be optimized.

According to the Hall-Petch relation, grain refinement is the most reliable method for enhancing mechanical properties of metals and alloys [3-5]. Highly strained metallic materials can possess not only an ultrafine-grained (UFG) structure but also specific nanostructural features [6-8]. To date, it is well established that bulk nanostructured materials (BNMs) can be processed successfully through microstructural refinement using two basic methods of intense plastic deformation: (i) high pressure torsion [9]; (ii) equal channel angular pressing [10]. Over the last decade, there was emerged a wide variety of new techniques of intense plastic deformation such as (i) accumulative roll bonding (ARB) [11]; (ii) multiaxial forging [12]; twist extrusion [13]; and many others. However, equal channel angular pressing still remains the most efficient technique producing large scale pieces of nanostructured materials. Nanostructured Ti and its alloys are of high potential employment for biomedical applications [14-17]. Pure titanium possesses the highest biocompatibility with living organisms, but it has limited use in medicine due to its low strength. High-strength nanostructured pure Ti processed by ECAP has already been exercised for biomedical application [5]. The main advantage of pure titanium is that toxic alloying elements are not present in the titanium implants and therefore such implants exhibit better biocompatibility with human body.

It is widely accepted that four or more passes of ECA pressing via route Bc are sufficient to achieve homogeneous ultrafine-grained microstructure in any cross-sections of the titanium billet. Tailoring ho-

Corresponding author: Alexander Zhilyaev, e-mail: AlexZ@anrb.ru

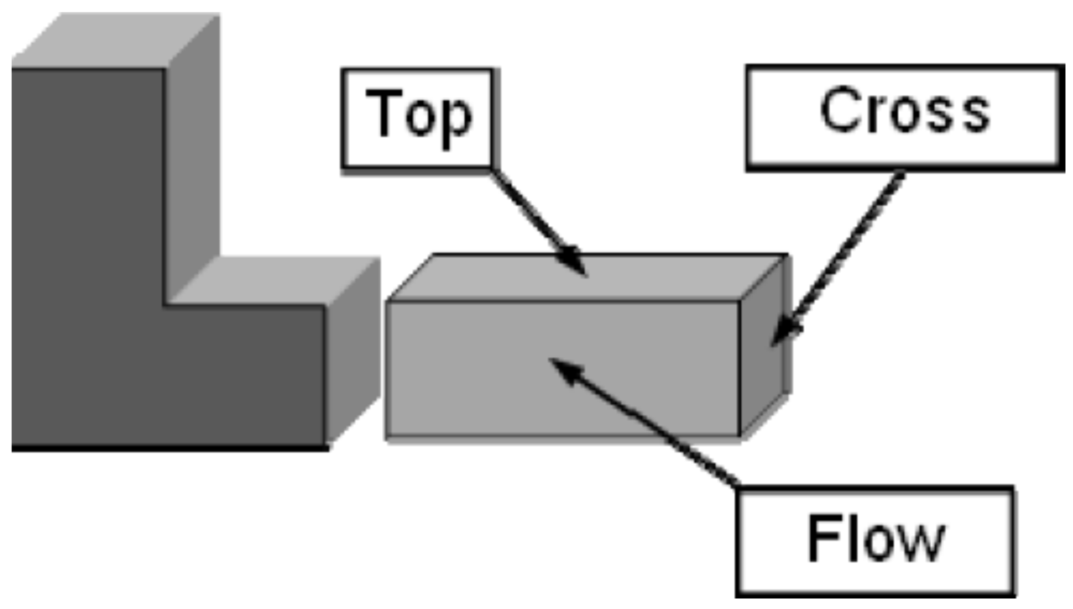

Fig. 1. Schematic of ECAP processing and flow and top planes and cross section analyzed.

mogeneity of microstructure is important to control mechanical properties of ECAP titanium during consequent thermomechanical treatment of the specimen during a fabrication of articles suitable for biomedical applications. For example, ECAP samples of pure titanium can be subjected to additional cold rolling for processing flat samples or warm drawing for obtaining rod-shaped specimens. Although there are a number of reports (see for references [8,18]) devoted to evolution microstructure and microtexture of titanium and Ti alloys during ECAP and few reports are consequent cold rolling of ECAP specimens [19-21]. The aim of current report is to reexamine a 3D homogeneity of microstructure and texture in ECAP titanium after eigth passes via route Bc processed at T = 450 °C.

2. MATERIALS AND EXPERIMENTAL

Commercially pure Ti (in Russian designation VT-1-0) with an average grain size greater than 10 μm and containing impurities including 0.12 wt.% O, 0.01 wt.% H, 0.04 wt.% N, 0.07 wt.% C, and 0.18 wt.% Fe was used as the starting material. Rectangular specimens were pressed through ECAP 90° die using route B_C, which consists of consequence of rotations of the work piece 90° clockwise along its longitudinal axis between adjacent passes, was used to process the Ti billets. Molybdenum disulfide was used as a lubricant. Both Ti billet and die were preheated to 450 °C prior the first ECAP pass. Two samples were processed for eight passes, with the starting temperature at 450 °C. The temperature decreased with each pass and reached 400 °C after the 8th pass.

Vickers microhardness maps were plotted using microhardness data recorded in three sections of ECAP specimens (Fig. 1) on grid with step size of about 1 mm. Load of 100 gf and dwelling time of 15 s were employed for all Hv measurements.

TEM study of the Ti samples was carried out by transmission electron microscope JEM-2000EX. The foils were prepared by jet electropolishing. Thin foils for the study were obtained by Jet polishing using "Tenupol-5" in 6% $HClO_4$ solution of methanol and n-butanol, at a voltage of 40 V at a temperature of –35 °C. All details can be found elsewhere [22].

The XRD analyses were carried out by DRON-3 instrument equipped with monochromator using Cu radiation ($K_{\alpha 1}$ = 1.54060 Å). The scan step was 0.02°, and the exposure time was 2.5 s. Rietveld analysis using MAUD software [23] was performed in order to monitor the microcrystallite size, d; and the microstrain, $\langle\varepsilon^2\rangle^{1/2}$. Dislocation density has been estimated by the equation [24]:

$$\rho = \frac{3\sqrt{2\pi\left\langle \varepsilon^2 \right\rangle^{1/2}}}{d \cdot b},$$

where d is a crystallite size and b = 2.56 Å is the Burgers vector of α-titanium [25].

For texture analysis, about one third of the thickness was removed by mechanical polishing in order to exclude surface artifacts. Four incomplete pole figures $(10\bar{1}0)$, (0002), $(10\bar{1}1)$, $(10\bar{1}2)$ were measured by XRD in reflection geometry with Cu-K_α radiation.

3. RESULTS AND DISCUSSION

3.1. Microhardness maps

Fig. 2 represents color-coded (see online version) microhardness maps plotted in three sections: in flow plane (Fig. 2a), in top plane (Fig. 2b) and in the plane of the cross-section (Fig. 2c). In flow and top planes microhardness level is identical with the average value of ~ 2200 MPa. Surprisingly, in cross section average level of Hv is about 2050 MPa which is noticeable lower than in other planes. However, it shall be admitted that in the range of 10% error all the planes possess homogeneous microhardness. This consists with generally accepted belief that four passes of ECAP via route Bc is sufficient for achieving 3D microhardness homogeneity of processed billets [8,10]. Homogeneity of titanium processed up to four passes by 135 °ECAP via route Bc at room temperature has been studied in [26]. In the flow plane and the cross section of the ECAP billet the average microhardness values are higher due to room temperature deformation but they are identical and increase with increasing number of passes or accumulated strain.

3.2. TEM microstructure

Fig. 3 (upper row) represents typical microstructure in three planes of the ECAP billets. Middle row of

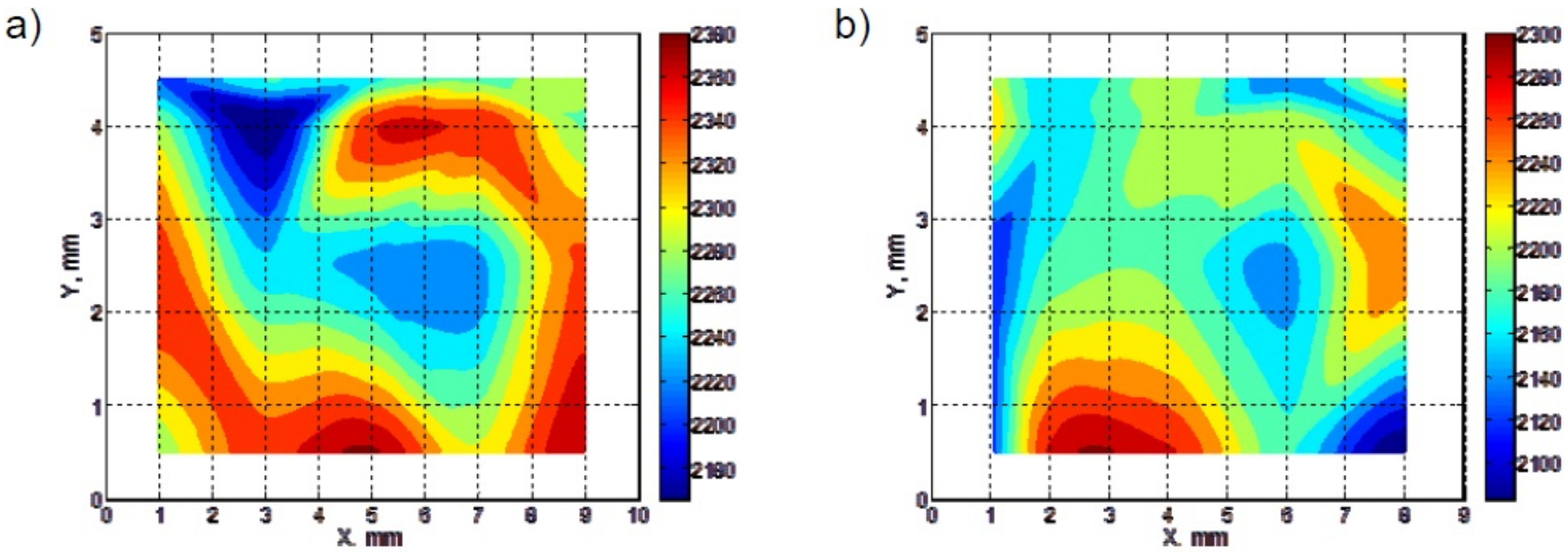

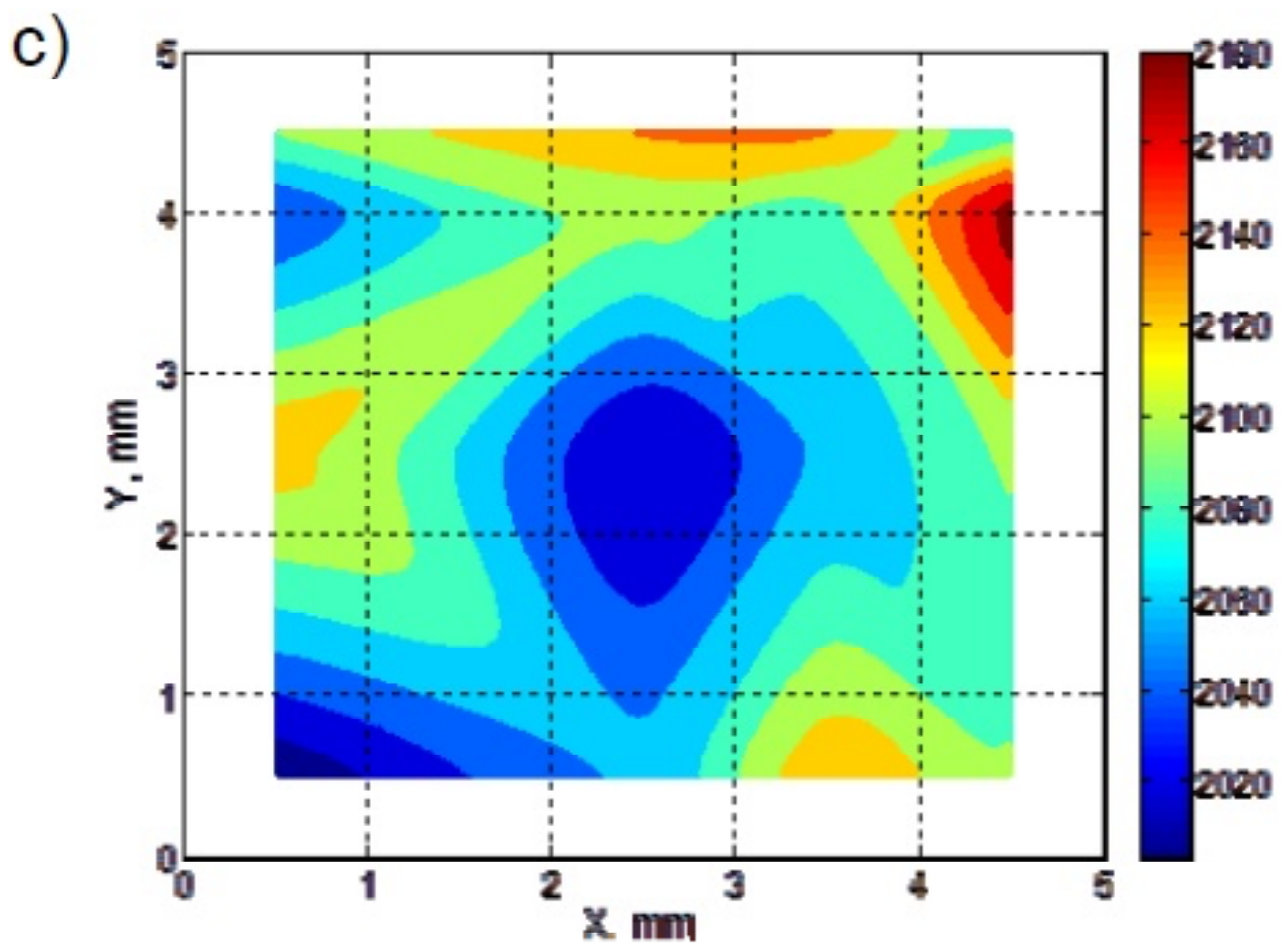

Fig. 2. Microhardness maps in (a) flow plane, (b) top plane and (c) cross section.

the Fig. 3 shows the distribution of longitudinal and transverse axes of grains from TEM observations. Last row of the Fig. 3 reflects the distribution of the aspect ratio of grains in three planes of the ECAP specimen. Average length of longitudinal/transverse axes of the grains is 0.51/0.22 μm in the flow plane, 0.49/0.25 μm in the top plane and 0.52/0.30 μm in the cross section, respectively. Average aspect ratios in three planes are 2.3, 2.1, and 1.8. However, there is no directional elongation of grains detected in any planes under study. Mean grain sizes of the ECAP titanium calculated in different planes are 0.37 μm, 0.37 μm, and 0.41 μm. They correlate with the average microhardness values measured in the same planes.

3.3. Crystallite size and dislocation density measured by XRD

Fig. 4a demonstrates a difference in the lattice parameters (*a* and *c*) of ECAP titanium in three planes. For comparison lattice parameters of annealed Ti specimen are shown. Apparently there is no significant change in parameters *a* in three planes and it is close to one of annealed sample. Long lattice axis, *c*, is smaller than that for annealing condition but it is similar in three different sections. Fig. 4b shows the crystallite size and the dislocation density calculated in the flow, top planes and in the cross-section. For comparison filled circles represent a mean grain size from TEM data in three sections. It is evident that crystallite size (actually subcells size) decreases in order of the flow plane → the top plane → the cross section. Mean grain size in all three planes is close to sub-cells size of the annealed specimen.

3.4. Texture homogeneity

Fig. 5 represents complete pole figures $(10\bar{1}0)$, (0002), $(10\bar{1}1)$, $(10\bar{1}2)$ in three planes (Figs. 5a, 5b, and 5c). Fig. 5d shows pole figures rotated 90° from the cross section to coincide the flow plane. Fig. 5e presents pole figures rotated for 45° from the cross section to coincide the the shear plane of the ECAP die. Insets in Fig. 5 show the texture maximum for each plane. There is no much difference in texture maxima in the different planes of the ECAP billets which is a good indication of the crystallographic isotropy. Rotated 90° pole figures of that recorded in cross section (Fig. 5d) are in good agreement with pole figures obtained from the top plane (Fig. 5b). Actually from statistics point of view they are identical.

Pole figures rotated 45° from the cross section to coincide to the shear plane of the ECAP billet

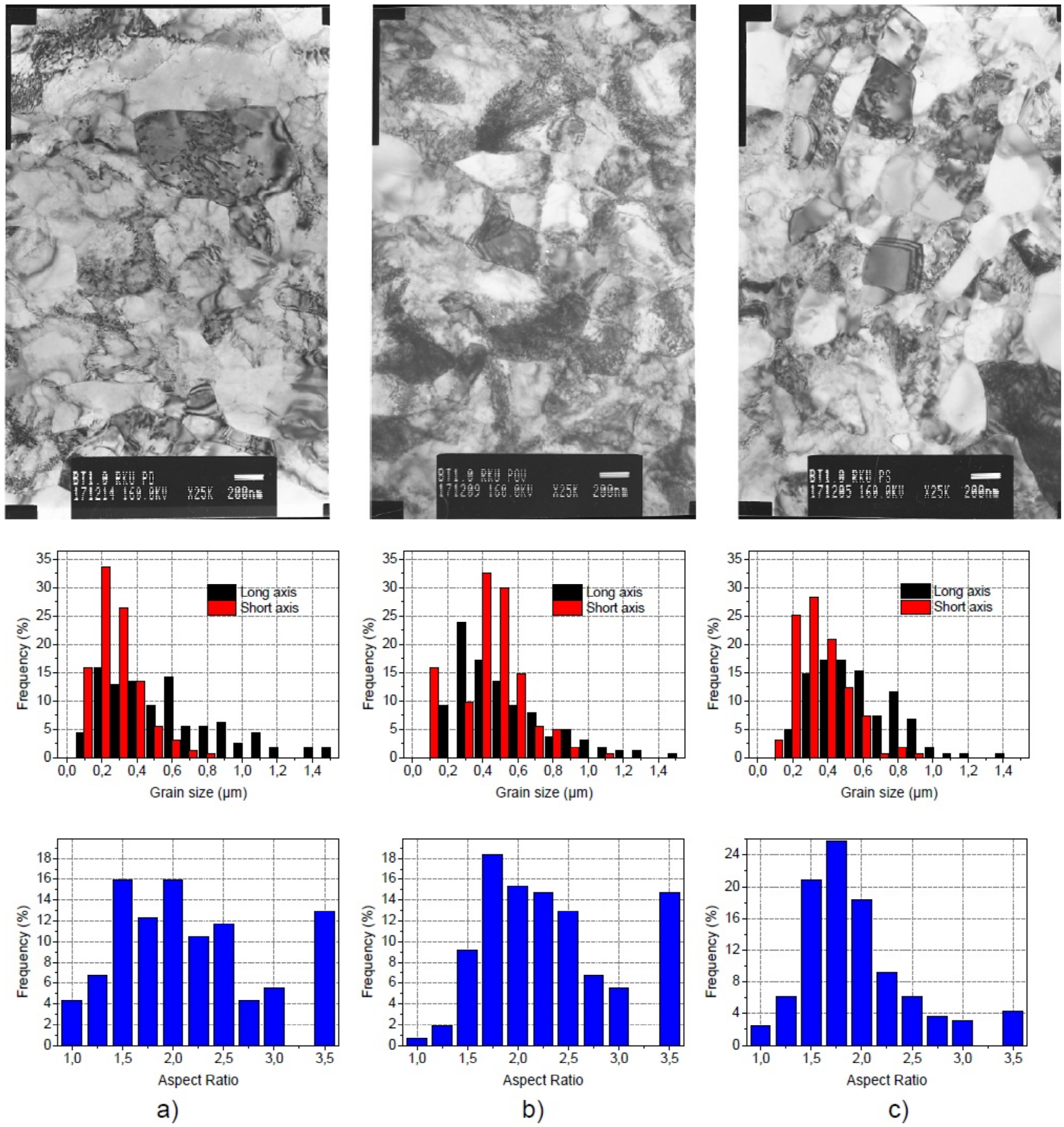

Fig. 3. TEM microstructure (upper row), grain size distribution in long and short axes (middle row) and axis ratio distribution (bottom row) in (a) flow plane, (b) top plane and (c) cross section.

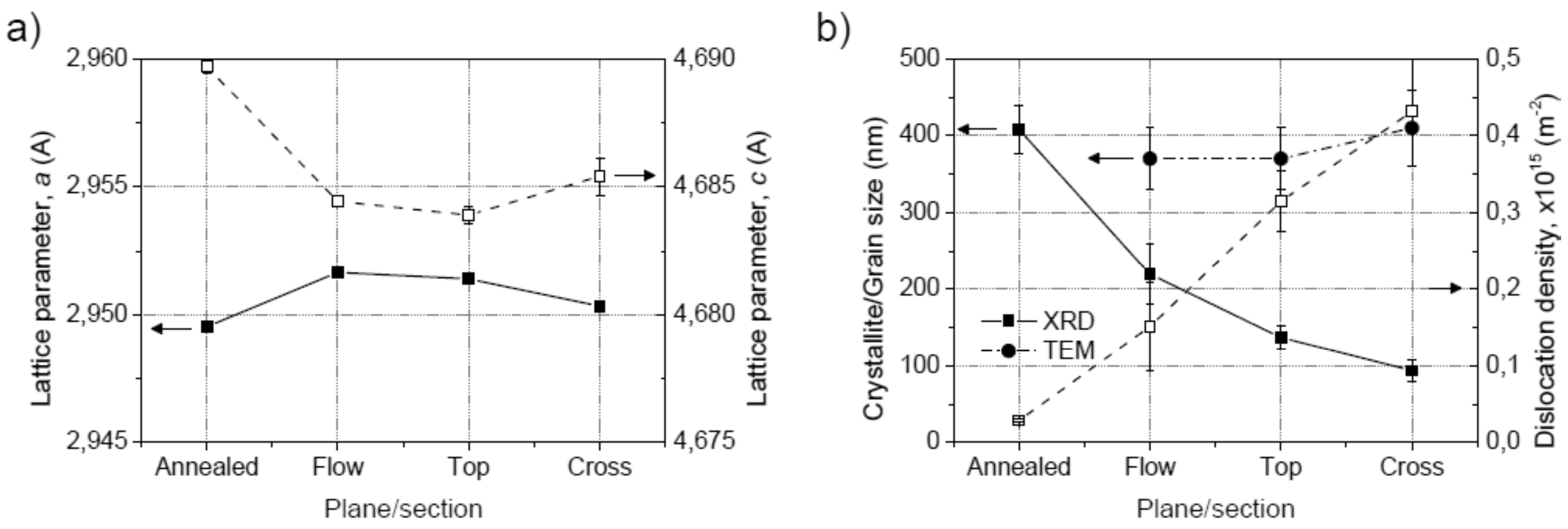

Fig. 4. (a) Lattice parameters (*a* and *c*) and (b) Crystallite/Grain size and dislocation density evaluated from TEM and XRD data.

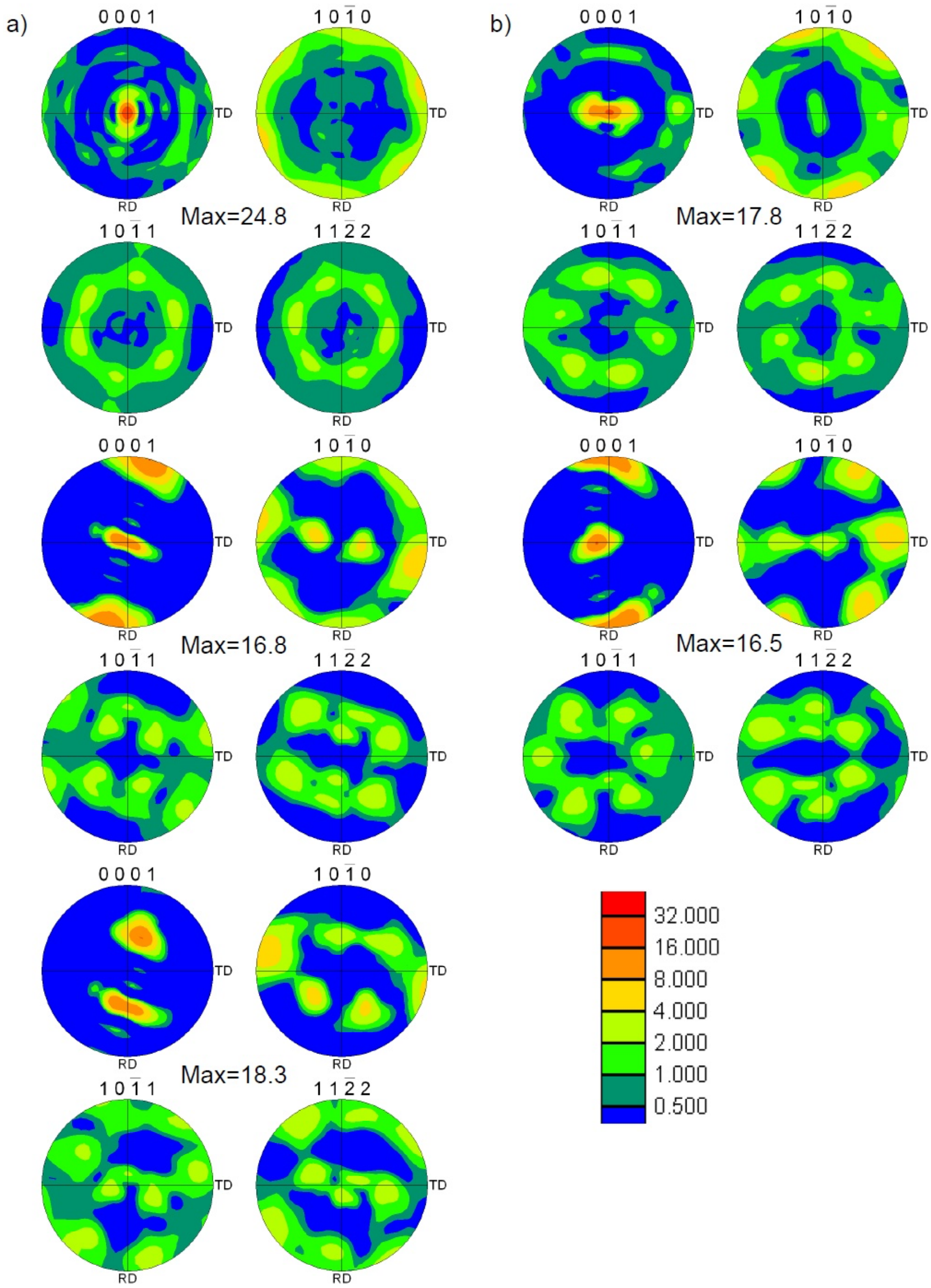

Fig. 5. Pole figures, measured in (a) flow plane, (b) top plane and (c) cross section; (d) PFs rotated 90° from cross section plane to coincide to flow plane; e) PFs rotated 90° from cross section plane to coincide to shear plane of ECAP die.

gives the indication of active slip systems during processing. They are pyramidal <c+a> (11$\bar{2}$2)[11$\bar{2}$3] slip system and (10$\bar{1}$1) compression twinning. This is in good agreement with experimental slip systems reported elsewhere [18,27].

4. CONCLUDING REMARKS

Equal channel angular pressing of commercially pure titanium via route Bc for eight passes leads to 3D homogeneous microstructure in mean grain size and texture. Sub-cell structure is finer in the cross section of the ECAP billet and shows enhanced dislocation density comparing to the flow and top planes.

ACKNOWLEDGEMENTS

This work was supported by Russian Science Foundation under Grant #14-29-00199.

REFERENCES

[1] T*itanium and Titanium Alloys: Fundamentals and Applications*, ed. by C. Leyens and M. Peters (Weinheim, Wiley-VCH Verlag GmbH, 2003).

[2] U.F. Kocks, C.N. Tome and H.R. Wenk, *Texture and anisotropy* (Cambridge, Cambridge University Press, 1998).

[3] R.Z. Valiev, R.K. Islamgaliev and I.V. Alexandrov // *Prog. Mater. Sci*. **45** (2000) 103.
[4] H. Gleiter // *Acta Mater.* **48** (2000) 1.
[5] R.Z. Valiev, I. Sabirov, A.P. Zhilyaev and T.G. Langdon // *JOM* **64** (2012) 1134.
[6] B. Baretzky, M.D. Baro, G.P. Grabovetskaya, J. Gubicza, M.B. Ivanov, Yu.R. Kolobov, T.G. Langdon, J. Lendvai4, A.G. Lipnitskii, A.A. Mazilkin, A.A. Nazarov, J. Nogues, I.A. Ovidko, S.G. Protasova, G.I. Raab, A. Revesz, N.V. Skiba, J. Sort, M.J. Starink, B.B. Straumal, S. Surinach, T. Ungar and A.P. Zhilyaev// *Rev. Adv. Mater. Sci.* **9** (2005) 45.
[7] R.Z. Valiev, Y. Estrin, Z. Horita, T.G. Langdon, M.J. Zehetbauer and Y.T. Zhu // *JOM* **5**8 (2006) 33.
[8] R.Z. Valiev, A.P. Zhilyaev and T.G. Langdon, *Bulk nanostructured materials: Fundamentals and applications* (New Jersey, Wiley & Sons, 2014).
[9] A.P. Zhilyaev and T.G. Langdon // *Prog. Mater. Sci*. **53** (2008) 893.
[10] R.Z. Valiev and T.G. Langdon // *Prog. Mater. Sci.* **51** (2006) 881.
[11] Y. Saito, N. Tsuji, H. Utsunomiya, T. Sakai and R.G. Hong // *Scripta Mater.* **39** (1998) 1221.
[12] O.R. Valiakhmetov, R.M. Galeyev and G.A. Salishchev // *Fiz. Metall. Metalloved.* **10** (1990) 204.
[13] D.V. Orlov, V.V. Stolyarov and H. Sh. Salimgareyev, In: *Ultrafine Grained Materials III*, ed. by Y.T. Zhu, T.G. Langdon, R.Z. Valiev, S.L. Semiatin, D.H. Shin and T.C. Lowe (Warrendale (PA), TMS; 2004), p. 457.
[14] S. Faghihi, A.P. Zhilyaev, J.A. Szpunar, F. Azari, H.Vali and M. Tabrizian // *Adv. Mater.* **19** (2007) 1069.
[15] S. Faghihi, F. Azari, A.P. Zhilyaev, J.A. Szpunar, H.Vali andM. Tabrizian // *Biomaterials* **28** (2007) 3887.
[16] R.Z. Valiev, I.P. Semenova, V.L. Latysh, H. Rack, T.C. Lowe, J. Petruzelka, L. Dluhos, D. Hrusak and J. Sochova // *Adv. Eng. Mater.* **10** (2008) B15.
[17] Y. Estrin, E.P. Ivanova, A. Michalska, V.K. Truong, R. Lapovok and R. Boyd // *Acta Biomater.* **7** (2011) 900.
[18] I.J. Beyerlein and L.S. Tóth // *Prog. Mater. Sci.* **54** (2009) 427.
[19] S.V. Zherebtsov, G.S. Dyakonov, A.A. Salem, S.P. Malysheva, G.A. Salishchev and S.L. Semiatin // *Mater. Sci. Eng. A* **528** (2011) 3474.
[20] S. Mironov, M. Murzinova, S. Zherebtsov, G.A. Salishchev and S.L. Semiatin // *Acta Mater.* **57**(2009) 2470.
[21] B. Beausir, L.S. Tóth and K.W. Neale // *Acta Mater.* **55** (2007) 2695.
[22] A.P. Zhilyaev, V.A. Popov, A.R. Sharafutdinov and V.N. Danilenko // *Let. Mater.* **1** (2011) 203.
[23] http://www.ing.unitn.it/maud/
[24] R.E. Smallman and K.H. Westmacott // *Philos. Mag.* **2** (1957) 669.
[25] A.P. Zhilyaev, S.N. Sergeev, V.A. Popov and A.V. Orlov // *Rev. Adv. Mater. Sci.* **39** (2014) 15.
[26] L. Xiaoyan, Z. Xicheng, Y. Xirong, J. Jiangping and Q. Boli // *J. Wuhan Uni. Tech.-Mater. Sci. Ed.* **29** (2014) 578.
[27] J. Bonarski and I.V. Alexandrov, In: *Nanomaterials by Severe Plastic Deformation*, ed. by M. Zehetbauer and R. Valiev (Weinheim, Wiley-VCH Verlag GmbH, 2003).